Excitation Spectrum of the Toda Lattice: A Molecular-Dynamics Study

T. Schneider and E. Stoll
IBM Zurich Research Laboratory, CH-8803 Rüschlikon, Switzerland
(Received 19 May 1980)

With use of molecular-dynamics technique for the classical Toda lattice, phonon, soliton, and second-sound excitation branches have been found.

PACS numbers: 63.70.+h

The Toda lattice, proposed more than a decade ago,[1] is a one-dimensional string of equal masses with an exponential spring between pairs of nearest neighbors. The Hamiltonian (after appropriate scaling) is[2]

$$H=\sum_{l=1}^{N}\{\tfrac{1}{2}\dot{x}_l^2+\exp[-(x_{l+1}-x_l)]+x_{l+1}-x_l-1\}, \tag{1}$$

where $\dot{x}_l=dx_l/dt$ denotes the momentum, and x_l the displacement of the lth particle. In the intervening years, the Toda lattice has proved itself as the discrete counterpart of numerous nonlinear continuous systems admitting soliton solutions and having many conserved quantities beyond momentum and energy.[2-4]

Recently, there has been growing interest in the statistical mechanics of soliton-bearing systems[5] to identify soliton effects in the thermodynamic properties[6,7] and the dynamic linear-response functions.[8,9] In view of this, the Toda lattice is likely to become the standard model on which our understanding of the statistical mechanics of nonlinear lattices will have to be built in the future.

In this Letter, we present molecular-dynamics (MD) results for the Toda lattice. Assuming the establishment of thermal equilibrium, we concentrate on dynamic form factors which are the most revealing properties to unravel the excitation spectrum. Because of the lack of a firmly based theory for the classical statistical mechanics of dynamic properties in this system, the present work provides the first solid basis for a confrontation with approximate treatments. We studied a system with $N=10^3$ subjected to periodic boundary conditions defined by

$$x_{l+N}-x_l=N\Delta r, \tag{2}$$

Δr being the thermal expansion. Noting that the partition function can be calculated exactly,[2] the zero-pressure value of Δr is given by

$$\Delta r=\ln(1/T)-\psi(1/T), \tag{3}$$

where T denotes the temperature and ψ the digamma function. The equations of motion associated with Hamiltonian (1),

$$-\ddot{x}_l=e_l-e_{l-1}, \tag{4}$$

where

$$e_l=\exp[-(x_{l+1}-x_l)], \tag{5}$$

were integrated by using the Verlet algorithm[10] and a time step of 0.028. We started our studies with a well-equilibrated system and a prechosen average temperature, simply given by the kinetic energy. Dynamic form factors $S_{AA}(q,\omega)$ were computed from

$$A(q,t)=N^{-1/2}\textstyle\sum_l[A_l(t)-\langle A_l\rangle]\exp(iqal) \tag{6}$$

by calculating the correlation function

$$S_{AA}(q,t)=\langle A(q,t)A(-q,0)\rangle \tag{7}$$

and the Fourier transform

$$S_{AA}(q,\omega)=2\int_0^\infty S_{AA}(q,t)\exp(i\omega t)\,dt, \tag{8}$$

with q denoting the wave number. Assuming establishment of thermal equilibrium, the microcanonical averages indicated by angular brackets were estimated in terms of time averages. We considered the variables

$$x_l, H_l, \tag{9}$$

$$e_l=\exp[-(x_{l+1}-x_l)],\quad T_l=\tfrac{1}{2}\dot{x}_l^2, \tag{10}$$

$$\rho(q,t)=N^{-1/2}\textstyle\sum_l\{\exp[iqx_l(t)]-\langle\rangle\}. \tag{11}$$

H_l is the local energy defined by Eq. (1) and $H=\sum_l H_l$, and $\rho(q,t)$ describes the density fluctuations. The variable e_l and the kinetic energy T_l are simply related to the one-soliton solution of Eq. (4) (Ref. 2):

$$e_l=1+\sinh^2\alpha\,\operatorname{sech}^2(\alpha l\pm t\sinh\alpha), \tag{12}$$

$$T_l=\tfrac{1}{2}\sinh^2\alpha\{\tanh(\alpha l\pm\alpha vt)-\tanh[\alpha(l+1)\pm\alpha vt]\}^2, \tag{13}$$

α being an arbitrary constant and

$$v = \alpha^{-1} \sinh\alpha \tag{14}$$

the velocity of the soliton.

Before turning to the MD results for the associated dynamic form factors, we briefly sketch some approximate and exact results to calibrate the discussion. By expanding the variables ρ [Eq. (11)] and e [Eq. (10)] in terms of the displacements, a Hartree-type linearization of the equation of motion [Eq. (4)] yields

$$S_{\rho\rho}(q,\omega) \approx q^2 a^2 S_{xx}(q,\omega) = (Tq^2a^2\pi/\omega_q^2)[\delta(\omega+\omega_q)+\delta(\omega-\omega_q)], \tag{15}$$

$$S_{ee}(q,\omega) \approx \pi T[\delta(\omega+\omega_q)+\delta(\omega-\omega_q)], \tag{16}$$

where the phonon frequency ω_q is given by

$$\omega_q^2 = 2[1-\cos(qa)]. \tag{17}$$

These expressions are valid in the limit $T \to 0$, where the displacements become arbitrarily small. Because energy is conserved, we also expect a hydrodynamic mode in $S_{HH}(q,\omega)$ in terms of a resonance at small q due to second sound or heat diffusion. Using the Kwok estimate for the second-sound frequency,[11] we obtain, in one dimension and with the phonon frequency given by Eq. (17), the expression

$$\omega_{ss}^2(q) = 3.83 q_{\mathrm{red}}^2, \quad q_{\mathrm{red}} = qa/\pi. \tag{18}$$

Second sound is expected to occur only in a temperature window, bounded from below by a temperature still guaranteeing the establishment of local equilibrium, and from above by umklapp processes tending to overdamp the mode.[11] The nonlinear soliton modes might be brought into play in terms of an ideal-soliton-gas approximation, yielding

$$S_{ee}(l,t) = \frac{1}{Z_s}\sum_{N=0}^{\infty}\frac{1}{N!}\prod_{j=1}^{N}\int dl_{0j}\int\frac{dP_j}{d\alpha_j}\exp(-\beta E_j)\,d\alpha_j\sum_j e(l_j+l_{0j},t)\,e(l_{0j},0), \tag{19}$$

where

$$P_j = 2\sinh\alpha_j, \quad E_j = 2(|\sinh\alpha_j|\cosh\alpha_j - |\alpha_j|), \tag{20}$$

Z_s being the partition function of the ideal soliton gas, and P_j and E_j denoting momentum and energy of the jth soliton initially at l_{0j}. With use of Eq. (12), $S_{ee}(q,\omega)$ can be evaluated analytically. The result is

$$\hat{S}_{ee}(q,\omega) = \frac{S_{ee}(q,\omega)}{S_{ee}(q,t=0)} = \frac{\pi}{q}\sum_{n=1}^{2}\frac{(\cosh\alpha_n)v_n^4\exp[-\beta E(\alpha_n)]\sinh^{-2}(q\pi/2\alpha_n)}{\int_{-\infty}^{+\infty}d\alpha\,(\cosh\alpha)v^4\exp[-\beta E(\alpha)]\sinh^{-2}(q\pi/2\alpha)}\left|\frac{\alpha_n}{v_n-\cosh\alpha_n}\right|, \tag{21}$$

with the α_n being the two solutions of

$$v = \omega/q = \alpha^{-1}\sinh\alpha, \tag{22}$$

predicting the occurrence of a non-Lorentzian soliton resonance for $\omega \geq q$ and small q values.

Exact results might be derived from the equation of motion (4) and the partition function. We found

$$\omega^4 S_{xx}(q,\omega) = 2[1-\cos(qa)]S_{ee}(q,\omega), \tag{23}$$

$$(2\pi)^{-1}\int_{+\infty}^{-\infty} S_{ee}(q,\omega)\,d\omega = T, \tag{24}$$

and

$$(2\pi)^{-1}\int_{+\infty}^{-\infty} S_{ee}(q,\omega)\omega^2\,d\omega = 2T[T+(1-\cos(qa))]. \tag{25}$$

These relations are very useful to test approximations and the MD results.

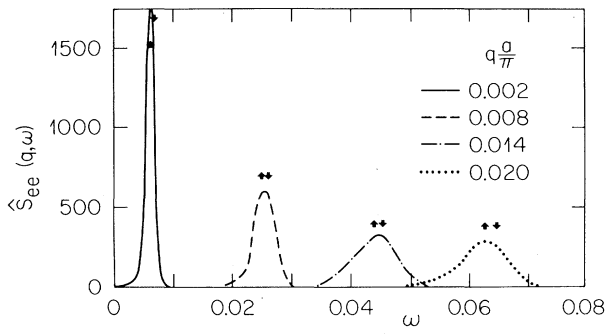

FIG. 1. $\hat{S}_{ee}(q,\omega)$ for a few selected q values at $T = 0.25$, and energy $E = 0.262$. The peak positions of the approximate treatments are marked by arrows: downward arrows, ideal-soliton-gas approximation [Eq. (21)]; upward arrows, phonon approximation [Eq. (17)].

We are now prepared to discuss the MD results. In Fig. 1, $\hat{S}_{ee}(q,\omega)$ is shown for a few selected q values at $T=0.25$. This temperature belongs to the low-temperature regime because the thermal expansion [Eq. (3)] is $\Delta r \approx 0.13$ only. The arrows mark the peak positions resulting from the phonon [Eqs. (16) and (17)] and ideal-soliton-gas approximations [Eq. (21)].

Within the limited ω resolution it is obviously not possible to separate the soliton from the phononlike contribution, because in the limit $q \to 0$, both tend to the dispersion law $\omega \approx q$. As shown in Fig. 2, an unambiguous identification in terms of a phononlike excitation branch becomes possible for larger q values, where the soliton contribution vanishes [Eq. (21)]. In fact, the dispersion law of the peak positions as determined by MD follow very closely the phonon expression [Eq. (17)]. It is important to note, however, that the phonon approximation does not account for the q dependence of the peak height [Eq. (16)] and that the ideal-soliton-gas approximation overestimates the soliton contribution expected at small q values. Since the dynamic form factors $S_{xx}(q,\omega)$, $S_{\rho\rho}(q,\omega)$, and $S_{ee}(q,\omega)$ are closely related [Eqs. (15) and (23)], they exhibit the same resonance structure. Thus, we also considered $S_{TT}(q,\omega)$ and $S_{HH}(q,\omega)$ to unravel the soliton contribution more clearly. Recognizing that $S_{ee}(q,\omega)$ was partially understood in terms of an interacting phonon gas, in $S_{HH}(q,\omega)$ we also expect a low-frequency resonance due to heat diffusion or second sound. Because the low-frequency resonance seen in Fig. 3 is well defined and its peak position agrees with the second-sound frequency estimate [Eq. (18)], we attribute these peaks to second sound.

The high-frequency resonance, however, is unexpected within the framework of a weakly anharmonic system, where second sound or heat diffusion exhausts the spectrum of $S_{HH}(q,\omega)$. On these grounds, we expect the high-frequency peak to be associated with solitons. To substantiate this conjecture, we also calculated the dynamic form factor $S_{TT}(q,\omega)$ [Eq. (10)] of the kinetic energy by MD and with the ideal-soliton-gas approximation. Here, e_l in Eq. (19) must be replaced by the one-soliton expression for T_l [Eq. (13)]. The resulting peak positions are marked in Fig. 3 and agree very well with the high-frequency resonance in $S_{HH}(q,\omega)$.

Accordingly, we attribute the excitation spectrum seen in Fig. 3 to second sound and soliton resonances.

We also performed MD calculations for $T=2.5$, corresponding to a rather high temperature, because the thermal expansion [Eq. (3)] is $\Delta r \approx 1.65$. Here $S_{ee}(q,\omega)$ exhibits a similar resonance structure, with considerably broader peaks, however. In $S_{HH}(q,\omega)$, second sound becomes overdamped and the soliton peaks are slightly broader.

These results show that the solitons of the Toda lattice do give rise to a new excitation branch in the dynamic form factors associated with the energy and kinetic-energy fluctuations. Moreover, we found a rather well-defined phonon excitation branch and second sound becoming overdamped at high temperatures. The results revealed, therefore, that the system can be viewed as a binary gas of interacting phonons and nearly free solitons. We hope that these results have opened a door on nonlinear phenomena which are absent

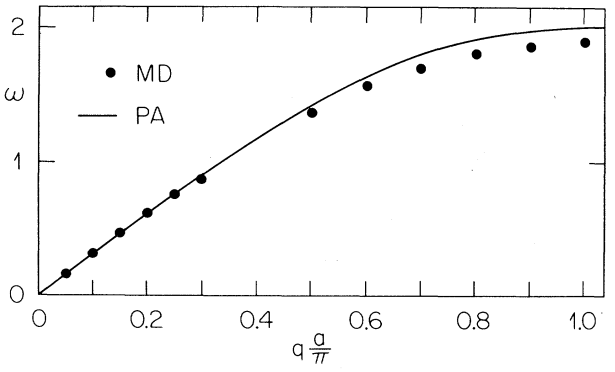

FIG. 2. Dispersion laws for the peak positions in $\hat{S}_{ee}(q,\omega)$ as obtained from MD and the phonon approximation (PA) [Eq. (17)].

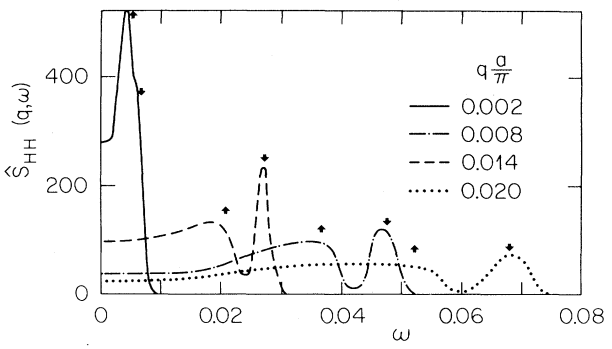

FIG. 3. $\hat{S}_{HH}(q,\omega)$ for a few q values at $T=0.25$. The arrows mark the peak positions of the approximate treatments: downward arrows, ideal soliton gas for $S_{TT}(q,\omega)$; upward arrows, second sound [Eq. (18)].

in nearly linear lattice dynamics.

[1]M. Toda, J. Phys. Soc. Jpn. 22, 431 (1967).
[2]M. Toda, Prog. Theor. Phys. Suppl. 45, 174 (1970).
[3]M. Toda, Rocky Mountain J. Math. 8, 197 (1978).
[4]A. C. Scott, F. Y. F. Chu, and D. W. McLaughlin, Proc. IEEE 61, 1443 (1973).
[5]*Solitons and Condensed-Matter Physics*, edited by A. R. Bishop and T. Schneider (Springer-Verlag, Berlin, 1978).
[6]A. R. Bishop, Phys. Scr. 20, 409 (1979).
[7]G. F. Mazenko and P. S. Sahni, Phys. Rev. B 18, 6139 (1978).
[8]T. Schneider and E. Stoll, Phys. Rev. Lett. 41, 1429 (1978).
[9]E. Stoll, T. Schneider, and A. R. Bishop, Phys. Rev. Lett. 42, 937 (1979), and 43, 405(E) (1979).
[10]L. Verlet, Phys. Rev. 159, 98 (1967).
[11]H. Beck, in *Dynamical Properties of Solids*, edited by G. K. Horton and A. A. Maradudin (North-Holland, Amsterdam, 1974), Vol. II, p. 205.

Observation of a Biaxial Nematic Phase in Potassium Laurate–1-Decanol–Water Mixtures

L. J. Yu and A. Saupe
Liquid Crystal Institute, Kent State University, Kent, Ohio 44242
(Received 9 June 1980)

The phase diagram of the ternary system potassium laurate–1-decanol–D_2O was studied over concentration ranges where nematic phases are likely to occur. Two uniaxial nematic phases which are separated by a biaxial nematic phase are found. In limited concentration range the following phase sequence may be observed reversibly on heating and on cooling: isotropic–uniaxial nematic (positive optical anisotropy)–biaxial nematic–uniaxial nematic (negative optical anisotropy)–biaxial nematic–uniaxial nematic (positive optical anisotropy)–isotropic.

PACS numbers: 64.70.Ew, 61.30.Gd, 76.60.Gv, 78.20.Fm

The existence of a uniaxial nematic phase with negative diamagnetic anisotropy in aqueous solutions of potassium laurate (KL) containing some 1-decanol and potassium chloride was first reported by Long and Goldstein.[1,2] The properties indicate that the phase has micelles of a bilayer structure. We denote this phase as N_L (see Refs. 3 and 4 for a discussion of structures and relations to Type-I and Type-II phases[5]). In studying the phase diagram of the ternary system KL–1-decanol–D_2O, we found that besides N_L two additional nematic phases occur. One of the additional phases is also uniaxial but of negative optical and positive diamagnetic anisotropy. It corresponds probably to a phase with cylindrical micelles and we denote it as N_C.[4] The third nematic phase occurs in concentration and temperature ranges that separate N_L and N_C. It is a biaxial nematic phase that we will denote as N_{bx}. To our knowledge this is the first time that the existence of a biaxial nematic phase has been clearly established.

The phases were classified by microscopic studies and by deuteron resonances as described in the following sections. Figure 1 shows part of the phase diagram of the KL–1-decanol–D_2O system. The 1-decanol concentration is constant at 6.24 wt. % while the weight concentration ratio of D_2O to KL varies from 2.67 to 2.56. For D_2O concentrations higher than 68 wt. % only one nematic phase N_L is formed. Upon cooling it transforms to a viscous isotropic phase and upon heating to an isotropic phase of a relatively low viscosity. The biaxial nematic phase N_{bx} is formed at 68 wt. % D_2O concentration. It transforms on cooling and on heating to N_L ($N_L \rightleftharpoons N_{bx} \rightleftharpoons N_L$). The N_C phase forms when the D_2O concentration is lowered to 67.8 wt. %. All three nematic phases occur near this concentration and the sequency by which they transform into each other is $N_L \rightleftharpoons N_{bx} \rightleftharpoons N_C \rightleftharpoons N_{bx} \rightleftharpoons N_L$. The range of N_C widens with decreasing water concentration whereas those of N_L and N_{bx} are narrowed. The N_C phase of the mixture with 67.4 wt. % D_2O transforms on heating directly to the isotropic micellar solution. Upon further heating a formation of batonnets takes place which may belong to a lamellar smectic phase.

Microscopic observations were made on the films sealed in flat capillaries. In general some

